Activation energy of alumina dissolution in FexO bearing slags

Taejun Kwack , Hyungsic Um , Yongsug Chung *

Posted Date: 8 September 2023

doi: 10.20944/preprints202309.0517.v1

Keywords: non-metallic inclusions; Al2O3 dissolution; activation energy; refining

Article

Activation Energy of Alumina Dissolution in FexO Bearing Slags

Taejun Kwack [1], Hyungsic Um [2] and Yongsug Chung [1,*]

[1] Department of Advanced Materials Engineering, Technical University of Korea, 237, Sangidaehak-ro, Shiheung-si, Gyeonggi-do, 15073, Republic of Korea

[2] R&D Center, Dongkuk Steel Company, 70, Geonposaneop-ro 3214beon-gil, Nam-gu, Pohang-si, Gyeongsangbuk-do, 37874, Republic of Korea

* Correspondence: ychung@tukorea.ac.kr

Abstract: The dissolution of Al_2O_3 non-metallic inclusions from slag containing Fe_xO was investigated in this study. The slag system used in the experiments was a quaternary system of CaO-SiO_2-Al_2O_3-Fe_xO. The composition of the slag was studied by fixing the basicity (CaO/SiO_2 ratio) to 1 and varying the Fe_xO content to 10 and 20 wt%. In addition, the experimental temperature was varied as 1550 °C, 1575 °C, and 1600 °C to study the effect of temperature on the Al_2O_3 dissolution behavior. The experimental equipment is a single hot thermocouple apparatus. The dissolution rate of Al_2O_3 particles increased linearly with increasing temperature and Fe_xO content. In addition, the mass transfer activation energy of Al_2O_3 dissolution in Fe_xO 10wt% and Fe_xO 20 wt% was calculated by an Arrhenius type analysis. The obtained mass transfer activation energies were 159 and 189 kJ/mole, respectively.

Keywords: non-metallic inclusions; Al_2O_3 dissolution; activation energy; refining

1. Introduction

In line with South Korea's 2030 carbon neutrality goal, the steel industry is also increasingly interested in electric arc furnaces, which emit less carbon dioxide than blast furnaces. Accordingly, research on electric arc furnace processes is necessary [1]. The electric arc furnace process injects oxygen into the steel to reduce operating time, oxidation refining, etc [2]. The presence of oxygen in the steel can cause problems such as corrosion and hot shortness. Therefore, a deoxidation process is essential [3]. The deoxidation process is mainly carried out using aluminum, which is a strong deoxidizer [4]. When tapping molten steel, aluminum is added to the ladle furnace to deoxidize it [5]. This process produces Al_2O_3 inclusions, which cause several problems including fatigue failure of the steel and nozzle clogging [6]. It is therefore important to remove Al_2O_3 inclusions as slag.

There are two ways to remove Al_2O_3 inclusions. The first is Ca treatment, where the Al_2O_3 inclusions are removed by adding Ca to transform the Al_2O_3 inclusion solid phase to a liquid CaO-Al_2O_3 phase [7]. However, this method has the disadvantage of interaction with the bottom lining refractory, which causes corrosion of the refractory. In addition, CaS inclusions, which are as harmful as Al_2O_3 inclusions, are easily formed [6]. The second is to float and separate Al_2O_3 inclusions to the slag/metal interface in a ladle refining process and then dissolve and remove them from the top layer of slag [8]. This method has been used not only in electric furnace processes, but also in blast furnace processes. For this reason, the dissolution behavior of non-metallic inclusions in slag has been extensively studied during the past 30 years.

Sridhar et al. [9] studied the dissolution behavior of Al_2O_3 particles in CaO-SiO_2-Al_2O_3-MgO slag with temperature as a variable. They reported that the dissolution of Al_2O_3 is dominated by mass transfer through the boundary layer. Q. Shu et al. [10] investigated the effect of Na_2O addition on the dissolution behavior of cylindrical Al_2O_3 in CaO-Al_2O_3-MgO-SiO_2 slag. They reported that the dissolution mechanism of Al_2O_3 is boundary layer mass transfer, and the dissolution rate of cylindrical Al_2O_3 increases with a decrease of slag viscosity and increase of thermodynamic driving force with Na_2O addition. Yi. K. Wi et al. [11] investigated the dissolution behavior of Al_2O_3 and MgO

particles within Al_2O_3-CaO-MgO slag, with temperature as the variable. Their research revealed that the dissolution kinetics of Al_2O_3 particles are primarily influenced by diffusion processes, whereas the dissolution of MgO particles adheres to chemical reaction kinetics. C. Ren et al. [12] examined how Al_2O_3 particles dissolve within CaO-Al_2O_3-SiO_2 slag, considering variations in slag composition and temperature. They reported that the rate-limiting step of Al_2O_3 particle dissolution in CaO-Al_2O_3-SiO_2 slag is diffusion in liquid slag, and an increase of C/A and C/S increased the dissolution rate of Al_2O_3 particles. L. Holappa et al. [13] studied the dissolution behavior of Al_2O_3 particles and $MgO \cdot Al_2O_3$ particles in CaO-SiO_2-Al_2O_3-MgO slag with basicity as a variable. They reported that Al_2O_3 particles and $MgO \cdot Al_2O_3$ particles dissolve slowly in slag with low basicity and the dissolution rate of the particles increases in slag with low viscosity. H. Um et al. [5] investigated the dissolution behavior of Al_2O_3 particles in CaO-SiO_2-Al_2O_3-Fe_xO slag with Fe_xO content as a variable. They reported that as the Fe_xO content increased from 0 to 20wt%, the dissolution rate of Al_2O_3 particles increased due to the decrease in viscosity. However, when the Fe_xO content increased to 30wt%, the dissolution rate did not increase due to the formation of the CA6 phase at the Al_2O_3 particle interface. Y. Park et al. [14] studied the dissolution behavior of wall-type Al_2O_3 in CaO-Al_2O_3-Fe_xO-MgO-SiO_2 slag with C/A and Fe_xO content as variables. They reported that increasing temperature, increasing C/A, and increasing Fe_xO content increased the dissolution rate of Al_2O_3. They also conducted temperature-variable experiments on slag having one composition to derive the mass transport activation energy of Al_2O_3 dissolution, which they reported to be 193.6 kJ/mole. S. Yeo et al. [15] conducted a study on the dissolution behavior of Al_2O_3 particles in CaO-Al_2O_3-SiO_2 slag with Al_2O_3 composition and temperature of the slag as variables. The investigators found that the dissolution rate increased with increasing activity of Al_2O_3. In addition, they reported that the diffusion activation energy of Al_2O_3 dissolution was in a range of about 320 to 490 kJ/mole depending on the composition of Al_2O_3 in the slag.

In addition, the dissolution behavior of Al_2O_3 in slags under various conditions has been studied [16–20]. However, since electric arc furnace slags use Fe scrap as raw material, the content of Fe_xO in the slag increases [2]. For this reason, the composition of the slag used in electric furnace research must include FexO. However, there has been little research on the dissolution behavior of non-metallic inclusions in slag containing Fe_xO. In addition, the temperature of electric arc furnace slag varies from 1550 °C to 1700 °C, but few studies have been conducted with temperature as a variable in slag containing Fe_xO [21]. For this reason, the dissolution behavior of Al_2O_3 particles in CaO-SiO_2-Al_2O_3-Fe_xO slag was studied in this work with temperature and Fe_xO content as variables.

2. Materials and Methods

2.1. Sample Preparation

Table 1 shows the chemical composition and diameter of the Al_2O_3 particles used in the experiment. The shape of Al_2O_3 particles is spherical, with a diameter of 500 ± 2.5 μm (Goodfellow Cambridge limited, Huntingdon, UK). The average weight of the particles was 0.25 mg and the purity of Al_2O_3 is 99.9%.

Table 1. Chemical compositions and diameter of Al_2O_3 particles.

Type	Source	Diameter	Weight	Concentration	
				Al_2O_3 (%)	Other (%)
Alumina sphere	GoodFellow	500 ± 2.5 μm	0.25 ± 0.05 mg	99.9	0.1

Table 2 shows the chemical composition and basicity of the slag used in the experiments. The basicity was fixed at 1, and the Fe_xO content was varied from 10 to 20 wt%. The amount of slag used in each experiment was set to 4mg for stability of the experiment. The slag was prepared by mixing

Preprints (www.preprints.org) | NOT PEER-REVIEWED | Posted: 8 September 2023 doi:10.20944/preprints202309.0517.v1

CaO powder prepared by calcining $CaCO_3$ at 1200 °C with Al_2O_3 and Fe_xO powder individually and melting them in a high frequency induction furnace.

Table 2. Chemical compositions of slag (wt%).

	CaO	SiO_2	Al_2O_3	Fe_xO	Basicity	References
Slag0	47.5	47.5	5	0	1	[9]
Slag1	42.5	42.5	5	10	1	
Slag2	37.5	37.5	5	20	1	
Slag3	32.5	32.5	5	30	1	[11]

2.2. Single Hot Thermocouple Apparatus (SHT Apparatus)

In this study, we observed the dissolution behavior of Al_2O_3 particles using a SHT apparatus. Figure 1 is a schematic diagram of the SHT apparatus. It consists of a B-type thermocouple to melt slag and dissolve Al_2O_3 particles, a DHT controller to control and check the temperature of the B-type thermocouple, a video camera to observe and record the dissolution behavior of Al_2O_3 particles in real time, and an optical microscope.

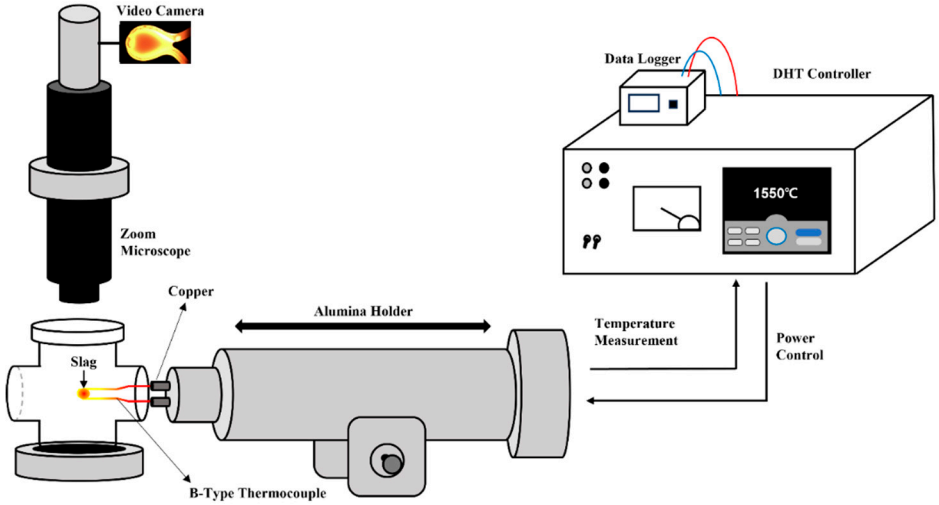

Figure 1. Schematic diagram of single hot thermocouple apparatus.

The SHT apparatus has several advantages, including the ability to inject Al_2O_3 particles at the desired temperature range, quenching at 300 °C/s using the DHT controller, ease of preparing quenching specimens, and real-time observation of the melting behavior of Al_2O_3 particles with a video camera and optical microscope.

2.3. Experimental Conditions

Figure 2 shows the process of the Al_2O_3 particle dissolution experiment using the SHT apparatus. First, the + and – poles of the B-type thermocouple are welded to form an oval shape, and then mounted on the copper tip. The slag is then placed on the B-type thermocouple and the temperature is raised to 8 °C/s using a DHT controller to melt the slag. When the experimental temperature (1550, 1575, 1600 °C) is reached, Al_2O_3 particles are added to the melted slag to dissolve it. Subsequently, after the setting time (120, 240, 360 sec), quenching was performed using the DHT controller.

Preprints (www.preprints.org) | NOT PEER-REVIEWED | Posted: 8 September 2023 doi:10.20944/preprints202309.0517.v1

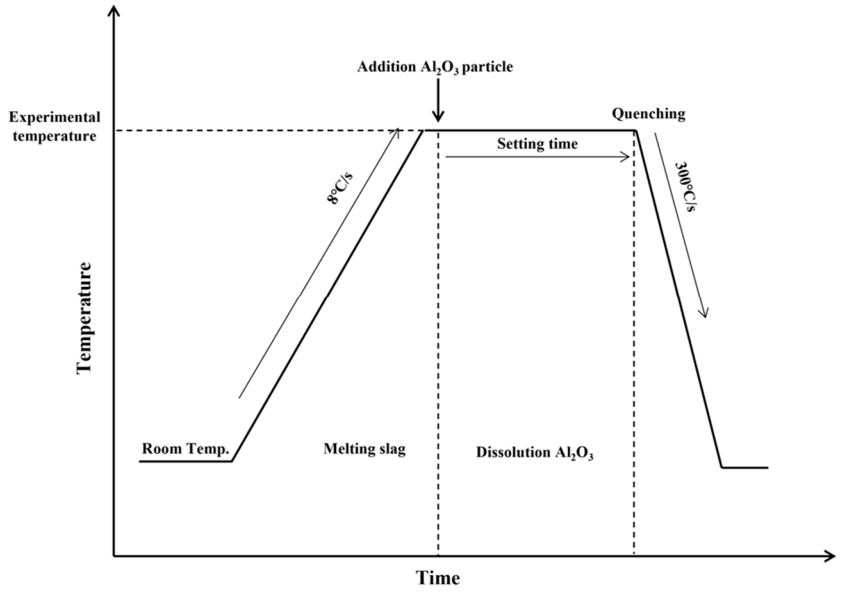

Figure 2. Experimental procedure of Al_2O_3 particle dissolution.

As mentioned earlier, the SHT apparatus has the advantage of allowing observation of the dissolution behavior of Al_2O_3 particles in real time. Several studies using this apparatus have taken advantage of this by observing the dissolution behavior of inclusions in real time [5,15,22,23]. However, in this study, there was a problem that the dissolution behavior of Al_2O_3 particles could not be observed in real time due to the opacity of the slag at high temperature because it contains Fe_xO, a transition metal. To solve this problem, in this experiment, quenching specimens were prepared by exploiting one of the advantages of the SHT apparatus, i.e., that quenching at 300 °C/s is possible. The quenching specimens were then polished and the diameter was measured in four directions, as shown in Figure 3a, to check the dissolution rate of Al_2O_3 particles. However, using this method, only a small portion of the diameter of the Al_2O_3 particles may be exposed. For this reason, the largest diameter value found by repeating the polishing several times was set as the representative value of the Al_2O_3 particle dissolution rate, as shown in Figure 3b.

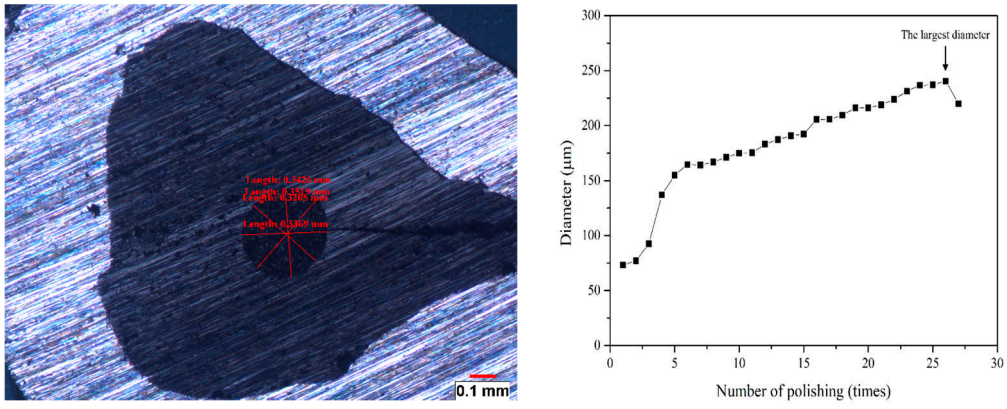

(**a**) (**b**)

Figure 3. Measurement of alumina diameter in opaque slag: (**a**) Measurement of Al_2O_3 particle in polished quenching specimens; (**b**) The largest diameter of Al_2O_3 particles found through multiple polishing.

The quenching specimens were also analyzed by SEM to identify the reaction layer at the interface between the slag and Al_2O_3 particles. No compounds were observed at the interface in the specimens.

Preprints (www.preprints.org) | NOT PEER-REVIEWED | Posted: 8 September 2023 doi:10.20944/preprints202309.0517.v1

3. Results and Discussion

3.1. Dissolution Behavior of Al_2O_3 Particles according to Temperature and Fe_xO content in Slag

The SHT apparatus was used to assess the dissolution behavior of Al_2O_3 particles in slag with changing Fe_xO content. The experiment temperatures were 1550, 1575, and 1600 °C, and the experiment times were 120, 240, and 360 seconds for each condition. Experiments were performed at least three times for each condition for reproducibility.

The variation of the diameter of Al_2O_3 particles in slags with different Fe_xO content at each temperature is shown in Figure 4. Slag0 and Slag3 are based on previous papers [5,15]. In the case of slag3, it was not possible to conduct experiments at temperatures above 1550 °C due to the short circuit of B-type thermocouples at high temperatures. Also, in the case of slag0, the temperature deviation was increased by 50 °C, and hence there are no data at 1575 °C.

Figure 4a shows the dissolution behavior of Al_2O_3 particles at 1550 °C. The diameter of the Al_2O_3 particles decreases linearly with the dissolution time, and the dissolution rate increases as the Fe_xO content in the slag increases. However, for slag3, the dissolution rate did not increase with increasing Fe_xO content. These experimental results are ascribed to the generation of the CA6 phase at the interface of Al_2O_3 particles and slag under the experimental conditions of slag3, which changed the dissolution process of the particles into an inter-compound chemical reaction [5]. Figure 4b shows the dissolution behavior of Al_2O_3 particles at 1575 °C. The results of the experiment at 1575 °C show that the diameter of the Al_2O_3 particles decreases linearly with the dissolution time, and the dissolution rate increases with an increase of Fe_xO content in the slag. Figure 4c shows the dissolution behavior of Al_2O_3 particles at 1600 °C. The results of the experiment at 1600 °C show that the diameter of the Al_2O_3 particles decreases linearly with the dissolution time, and the dissolution rate increases with an increase of Fe_xO content in the slag. However, at 1600 °C, in the slag2 experiment, the Al_2O_3 particles completely dissolved before 360 seconds. For this reason, additional experiments were conducted at 300 seconds for an accurate interpretation.

Table 3 lists the particle diameters of the Al_2O_3 particles for each condition.

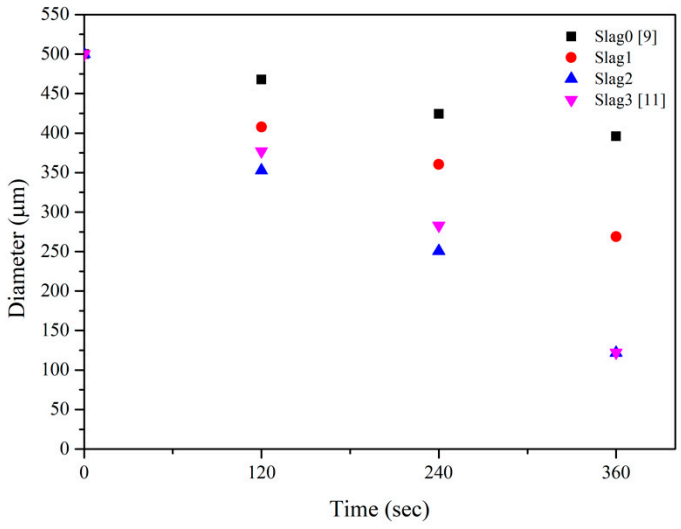

(a)

Preprints (www.preprints.org) | NOT PEER-REVIEWED | Posted: 8 September 2023 doi:10.20944/preprints202309.0517.v1

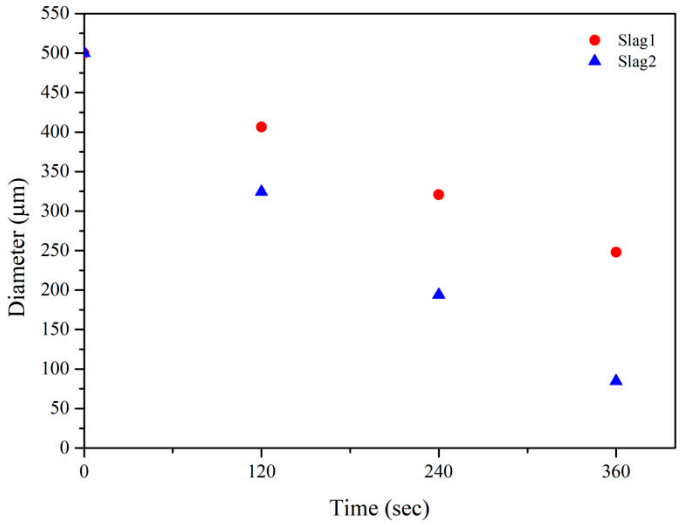

(**b**)

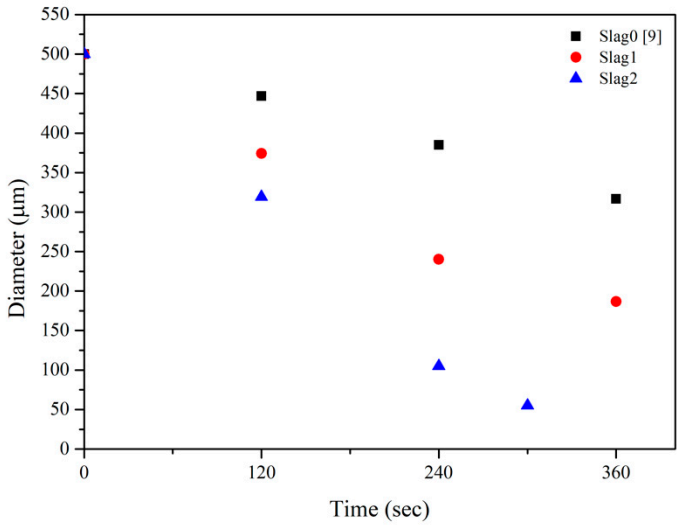

(**c**)

Figure 4. Al_2O_3 particle dissolution behavior according to Fe_xO content and temperature: (**a**) 1550 °C; (**b**) 1575 °C; (**c**) 1600 °C.

Table 3. Diameter of Al_2O_3 particles according to Fe_xO content and temperature (μm).

Temperature (°C)	Slag	120s	240s	360s	References
1550	0	465	420	393	[18]
	1	408	360	269	
	2	353	251	122	
	3	377	283	122	[5]
1575	1	407	321	248	
	2	324	194	85	
1600	0	447	385	317	[18]
	1	374	240	187	
	2	319	105	55 (300s)	

Preprints (www.preprints.org) | NOT PEER-REVIEWED | Posted: 8 September 2023 doi:10.20944/preprints202309.0517.v1

3.2. Analysis of Slag/Al_2O_3 Particle Interface by SEM

As previously described, H. Um et al. [5] reported that for slag3, a CA6 phase was created at the interface of slag and Al_2O_3 particles, which changed the dissolution process of Al_2O_3 particles. In addition, Park et al. [8] reported that a ring-shaped compound was formed along the particle/slag interface depending on the slag composition. For this reason, to better understand the dissolution behavior of Al_2O_3 particles in the experimental slag, the interface of slag and Al_2O_3 particles was analyzed by SEM. Figure 5 shows images of the interface of slag1, slag2, and Al_2O_3 particles under the condition of 1550 °C.

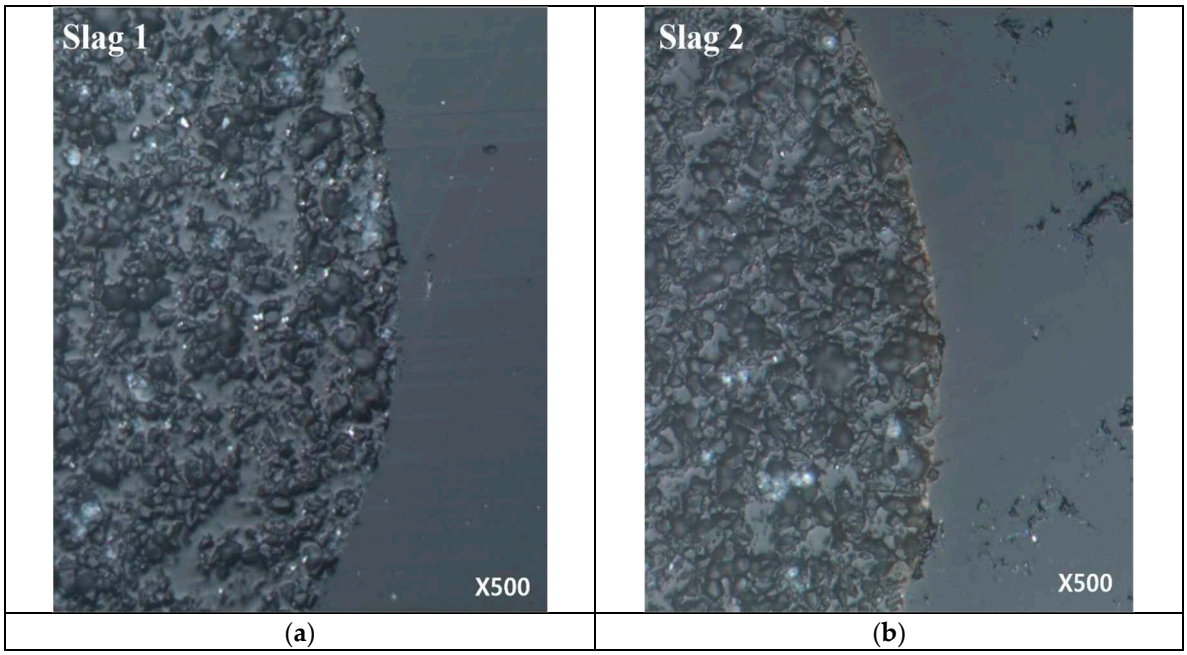

Figure 5. Cross-sectional image of Al_2O_3 particles by SEM: (**a**) Al_2O_3 particle in slag1; (**b**) Al_2O_3 particle in slag2.

It can be seen that no compounds are formed at the interface of slag1, 2, and Al_2O_3 particles. It was also confirmed that no compounds were formed at the interface at 1550°C or at 1575 °C and 1600 °C. S. Yeo et al. [15] and Taira et al. [24] reported that the dissolution rate of Al_2O_3 in CaO-SiO_2-Al_2O_3 slag is controlled by diffusion in the boundary layer. Also, H. Um et al. [5] reported that the dissolution of Al_2O_3 particles in CaO-SiO_2-Al_2O_3-Fe_xO slag is controlled by diffusion in the boundary layer of slag and Al_2O_3 particles if no compounds are generated at the interface of slag and Al_2O_3 particles. Therefore, it is believed that for the dissolution mechanism of Al_2O_3 particles in slag1 and slag2 it is only necessary to consider the behavior by diffusion in the boundary layer.

3.3. Dissolution Mechanism of Al_2O_3

Solid Al_2O_3 particles can be dissolved by liquid slag through the following process [5].

$$Al_2O_{3(s)} = Al_2O_{3(l)} \quad \ldots \quad \text{Chemical kinetics of the reaction at the interface} \tag{1}$$

$$Al_2O_{3(l)} = (Al_2O_3) \quad \ldots \quad \text{Liquid phase mass transfer} \tag{2}$$

In other words, the dissolution of solid Al_2O_3 particles in liquid slag can be controlled by a chemical reaction or liquid phase mass transfer [8,24–26]. It is interpreted that the dissolution of Al_2O_3 particles in liquid slag is controlled by liquid phase mass transfer in the boundary layer unless a compound is generated at the interface of Al_2O_3 particles and slag [9,27,28]. As noted above, no

Preprints (www.preprints.org) | NOT PEER-REVIEWED | Posted: 8 September 2023 doi:10.20944/preprints202309.0517.v1

compounds were generated at the interface of Al_2O_3 particles and slag under the present experimental conditions. Therefore, the rate-controlling step of Al_2O_3 particle dissolution in this experiment can be interpreted as liquid phase mass transfer at the boundary layer.

If the rate-controlling step in the dissolution of Al_2O_3 in slag is liquid phase mass transfer in the boundary layer, then the relationship between the mass transfer flux and mass transfer coefficient of Al_2O_3 particle dissolution can be expressed by the mass transfer equation as follows [29].

$$J = -k(C_i - C_b) \tag{3}$$

where J is the mass transfer flux; k is the mass transfer coefficient in the slag; C_i and C_b are the Al_2O_3 content at the interface and in bulk slag; and $(C_i - C_b)$ is the driving force of the dissolution.

If the Al_2O_3 particles being dissolved are spherical, then Equation (3) can be transformed into the following dissolution rate equation [29].

$$\frac{dr}{dt} = -k(C_i - C_b)M/\rho \tag{4}$$

where r is the radius of the Al_2O_3 particles; dr/dt is the dissolution rate; M is the molecular weight of Al_2O_3; and ρ is the slag density.

The dissolution rate can be calculated from the experimental data, as shown in Figure 6, and the slag density and driving force of the dissolution can be obtained using Factsage$^{7.3TM}$, and hence the mass transfer coefficient according to temperature and Fe_xO content can be derived using Equation (4). The physical properties and mass transfer coefficients for each temperature and Fe_xO content are summarized in Table 4.

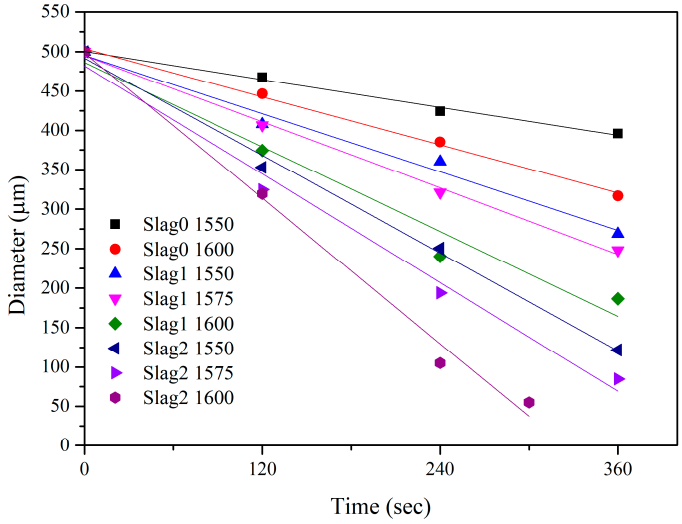

Figure 6. Dissolution rate by temperature and Fe_xO content.

Table 4. Physical properties and mass transfer coefficient according to temperature and Fe_xO content.

	Driving force of dissolution (ΔC) (mole/m³) *Factsage$^{7.3TM}$	**Slag density (ρ) (kg/m³)**	**Dissolution rate ($\frac{dr}{dt}$) (cm/s)**	**Mass transfer coefficient (k) (cm/s)**	**References**
Slag0 1550°C	10,745	2660	2.96×10^{-5}	7.19×10^{-8}	**[18]**
Slag0 1600°C	11,399	2647	5.10×10^{-5}	1.16×10^{-7}	

Preprints (www.preprints.org) | NOT PEER-REVIEWED | Posted: 8 September 2023 doi:10.20944/preprints202309.0517.v1

Slag1 1550℃	10,885	2796	6.18×10^{-5}	1.56×10^{-7}	
Slag1 1575℃	11,581	2789	7.01×10^{-5}	1.66×10^{-7}	Present study
Slag1 1600℃	11,846	2782	8.95×10^{-5}	2.06×10^{-7}	
Slag2 1550℃	11,050	2943	1.03×10^{-4}	2.69×10^{-7}	
Slag2 1575℃	11,600	2935	1.15×10^{-4}	2.84×10^{-7}	Present study
Slag2 1600℃	11,925	2928	1.65×10^{-4}	3.71×10^{-7}	

The mass transfer coefficient increases with the Fe_xO content in the slag and with increasing melting temperature.

3.4. Activation Energy

The activation energy of mass transfer, the dissolution mechanism of Al_2O_3, can be quantitatively measured. In this study, the dissolution rate of Al_2O_3 particles was measured with temperature as a variable, and the mass transfer coefficient was calculated accordingly. By graphing the reciprocal of the mass transfer coefficient and temperature using the Arrhenius equation, which is expressed as follows, the activation energy for mass transfer can be derived [30].

$$k = k_0 \cdot \exp\left(-\frac{E_k}{RT}\right) \tag{5}$$

where k is the mass transfer coefficient; k_0 is the pre-exponential constant; R is the universal gas constant; T is the absolute temperature; and E_k is the activation energy of mass transfer.

To explain how E_k is derived, substituting logarithms into the above expression, we can express it as a function of ln(k) and temperature, as follows.

$$\ln k = -\frac{E_k}{R}\frac{1}{T} + \ln k_0 \tag{6}$$

This expression tells us that the slope of the ln(k)-1/T graph is $-\frac{E_k}{R}$. Therefore, multiplying this value by -R gives the activation energy for mass transfer. Cho et al. calculated the mass transfer coefficient by measuring the dissolution behavior of Al_2O_3 in $CaO\text{-}SiO_2\text{-}Al_2O_3$ slag with temperature as a variable and derived the E_k of Al_2O_3 dissolution using the above method [29]. In this study, E_k was also calculated through the above process and is shown in Figure 7.

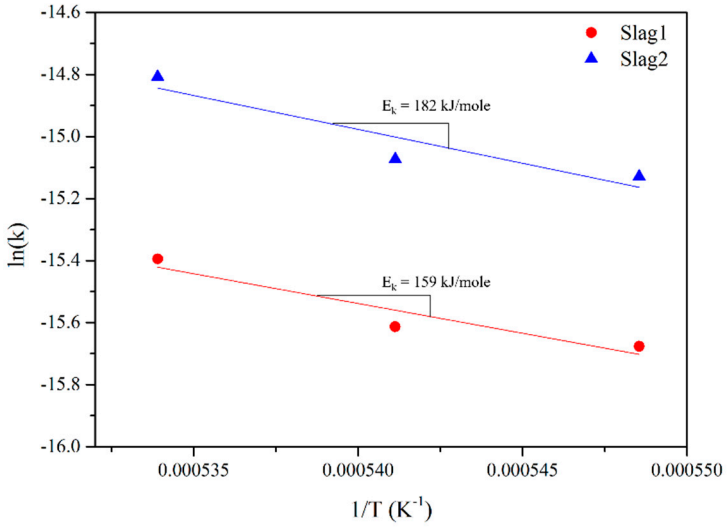

Figure 7. Arrhenius plot of the mass transfer coefficient.

Preprints (www.preprints.org) | NOT PEER-REVIEWED | Posted: 8 September 2023 doi:10.20944/preprints202309.0517.v1

The E_k of Slag1 was calculated to be 159 kJ/mole and the E_k of Slag2 was calculated to be 182 kJ/mole. In addition, the E_k of slag with Fe_xO calculated in this study and the E_k values of slag without Fe_xO calculated in other studies are summarized in Table 5.

Table 5. Comparison of Al_2O_3 dissolution E_k according to slag composition.

Slag	Chemical composition (wt%)						E_k (kJ/mole)	References
	CaO	SiO_2	Al_2O_3	MgO	Ce_2O_3	Fe_xO		
0	**47.5**	47.5	5.0	0	0	0	304	[15]
1	42.5	42.5	5.0	0	0	10	159	Present study
2	37.5	37.5	5.0	0	0	20	182	
4	45.0	10.0	45.0	0	0	0	445	[29]
5	35.0	30.0	35.0	0	0	0	334	
6	45.0	4.5	37.5	10.0	3	0	292	[31] [1]
7	45.0	4.5	35.5	10.0	5	0	347	
8	45.0	4.5	32.5	10.0	8	0	249	

[1] Cylindrical Al_2O_3 rotated at 200 rpm.

From Table 5, the E_k of the experimental slag with Fe_xO is lower than that of the slag without Fe_xO, indicating that the Al_2O_3 dissolution in the slag with Fe_xO is faster compared to that in the slag without Fe_xO.

4. Conclusions

In this study, the dissolution behavior of Al_2O_3 was studied by varying the Fe_xO content in the slag from 10 to 20wt% and the temperature as 1550 °C, 1575 °C, and 1600 °C. The results were as follows.

(1) The dissolution rate increased linearly as the Fe_xO content of the slag increased from 0 to 20 wt% and the dissolution temperature increased from 1550 to 1600 °C.
(2) Through a SEM analysis it was observed that no compound was formed at the interface of Al_2O_3 particles and slag. Therefore, the rate step of Al_2O_3 particle dissolution is interpreted as liquid phase mass transfer.
(3) The mass transfer coefficient was obtained using the dissolution rate equation. The mass transfer coefficient increased with increasing Fe_xO content in the slag and increasing dissolution temperature.
(4) The mass transfer coefficient is plotted in a graph as a function of temperature and the E_k values of slag1 and slag2 (159 and 182 kJ/mole, respectively) are found using the Arrhenius equation.
(5) The E_k of Al_2O_3 mass transfer in slag containing Fe_xO in this study was lower than the E_k of slag without Fe_xO.

Funding: This research was funded by the Korea Evaluation Institute of Industrial Technology (Grant number 1415188141, 1415188130), and by the Korea Institute of Energy Technology Evaluation and Planning (Grant number 1415187059).

Data Availability Statement: No data available.

Conflicts of Interest: The authors declare no conflict of interest.

References

1. Fan, Z., Friedmann, S.J., 2021. Low-carbon production of iron and steel: Technology options, economic assessment, and policy. Joule 5, 829–862. https://doi.org/10.1016/j.joule.2021.02.018
2. Lee, B., Sohn, I., 2014. Review of Innovative Energy Savings Technology for the Electric Arc Furnace. JOM 66, 1581–1594. https://doi.org/10.1007/s11837-014-1092-y
3. Park, J.H., Todoroki, H., 2010. Control of MgO. Al_2O_3 spinel inclusions in stainless steels. ISIJ Int. 50, 1333–1346. https://doi.org/10.2355/isijinternational.50.1333

4. Dimitrov, S., Weyl, A., Janke, D., 1995. Control of the aluminium-oxygen reaction in pure iron melts. Steel Res. 66, 3–7. https://doi.org/10.1002/srin.199501762
5. Um, H., Yeo, S., Kang, Y.-B., Chung, Y., 2022. The effect of FexO content on dissolution behavior of an alumina inclusion in CaO–Al_2O_3–SiO_2–FexO slag by a single hot thermocouple technique. Ceram. Int. 48, 35301–35309. https://doi.org/10.1016/j.ceramint.2022.08.132
6. Jung, I.-H., Decterov, S.A., Pelton, A.D., 2004. Computer applications of thermodynamic databases to inclusion engineering. ISIJ Int. 44, 527–536. https://doi.org/10.2355/isijinternational.44.527
7. Holappa, L., Hämäläinen, M., Liukkonen, M., Lind, M., 2003. Thermodynamic examination of inclusion modification and precipitation from calcium treatment to solidified steel. Ironmak. Steelmak. 30, 111–115. https://doi.org/10.1179/030192303225001748
8. Park, J.-H., Jung, I.-H., Hae-Geon, L.E.E., 2006. Dissolution behavior of Al_2O_3 and MgO inclusions in the CaO-Al_2O_3-SiO_2 slags: Formation of ring-like structure of $MgAl_2O_4$ and Ca_2SiO_4 around MgO inclusions. ISIJ Int. 46, 1626–1634. https://doi.org/10.2355/isijinternational.46.1626
9. Sridhar, S., Cramb, A.W., 2000. Kinetics of Al_2O_3 dissolution in CaO-MgO-SiO_2-Al_2O_3 slags: In situ observations and analysis. Metall. Mater. Trans. B Process Metall. Mater. Process. Sci. 31, 406–410. https://doi.org/10.1007/s11663-000-0059-2
10. Shu, Q., Zhang, X., Wang, Y., Li, J., Chou, K., 2015. Effect of Na_2O on dissolution rate of alumina in CaO-Al_2O_3-MgO-SiO_2 slag. Presented at the Proceedings of the 6th International Congress on the Science and Technology of Steelmaking, ICS 2015, pp. 606–609.
11. Yi, K.W., Tse, C., Park, J.-H., Valdez, M., Cramb, A.W., Sridhar, S., 2003. Determination of dissolution time of Al_2O_3 and MgO inclusions in synthetic Al_2O_3-CaO-MgO slags. Scand. J. Metall. 32, 177–184. https://doi.org/10.1034/j.1600-0692.2003.20631.x
12. Ren, C., Zhang, L., Zhang, J., Wu, S., Zhu, P., Ren, Y., 2021. In Situ Observation of the Dissolution of Al_2O_3 Particles in CaO-Al_2O_3-SiO_2 Slags. Metall. Mater. Trans. B Process Metall. Mater. Process. Sci. 52, 3288–3301. https://doi.org/10.1007/s11663-021-02256-w
13. Holappa, L., Kekkonen, M., Louhenkilpi, S., Hagemann, R., Schröder, C., Scheller, P., 2013. Active tundish slag. Steel Res. Int. 84, 638–648. https://doi.org/10.1002/srin.201200209
14. Park, Y.-J., Cho, Y.-M., Cha, W.-Y., Kang, Y.-B., 2020. Dissolution kinetics of alumina in molten CaO–Al_2O_3–Fe_tO–MgO–SiO_2 oxide representing the RH slag in steelmaking process. J. Am. Ceram. Soc. 103, 2210–2224. https://doi.org/10.1111/jace.16879
15. Yeo, S., Um, H., Chung, Y., 2021. The Effect of Alumina Activity on Dissolution Behavior of Alumina Particles in CaO–Al_2O_3–SiO2 Slags. Metall. Mater. Trans. B Process Metall. Mater. Process. Sci. 52, 3938–3945. https://doi.org/10.1007/s11663-021-02309-0
16. Zhang, S., Rezaie, H.R., Sarpoolaky, H., Lee, W.E., 2000. Alumina dissolution into silicate slag. J. Am. Ceram. Soc. 83, 897–903. https://doi.org/10.1111/j.1151-2916.2000.tb01291.x
17. Valdez, M., Prapakorn, K., Cramb, A.W., Seetharaman, S., 2001. A study of the dissolution of Al_2O_3, MgO and $MgAl_2O_4$ particles in a CaO-Al_2O_3-SiO_2 slag. Steel Res. 72, 291–297. https://doi.org/10.1002/srin.200100120
18. Monaghan, B.J., Chen, L., Sorbe, J., 2005. Comparative study of oxide inclusion dissolution in CaO-SiO_2-Al_2O_3 slag. Presented at the Ironmaking and Steelmaking, pp. 258–264. https://doi.org/10.1179/174328105X28793
19. Chen, G., He, S., Wang, Q., 2020. Dissolution behavior of Al2O3 into tundish slag for high-al steel. J. Mater. Res. Technol. 9, 11311–11318. https://doi.org/10.1016/j.jmrt.2020.07.107
20. Shi, G.-Y., Zhang, T.-A., Dou, Z.-H., Niu, L.-P., 2020. Dissolution behavior of Al_2O_3 inclusions in CaO-Al_2O_3 based slag representing aluminothermic reduction slag. Crystals 10, 1–12. https://doi.org/10.3390/cryst10111061
21. Odenthal, H.-J., Kemminger, A., Krause, F., Sankowski, L., Uebber, N., Vogl, N., 2018. Review on Modeling and Simulation of the Electric Arc Furnace (EAF). Steel Res. Int. 89. https://doi.org/10.1002/srin.201700098
22. Lee, S., Chung, Y., 2022. The effect of C content in MgO–C on dissolution behavior in CaO–SiO_2–Al_2O_3 slag. Ceram. Int. 48, 26984–26991. https://doi.org/10.1016/j.ceramint.2022.06.010
23. Kim, Y., Kashiwaya, Y., Chung, Y., 2020. Effect of varying Al2O3 contents of CaO–Al_2O_3–SiO_2 slags on lumped MgO dissolution. Ceram. Int. 46, 6205–6211. https://doi.org/10.1016/j.ceramint.2019.11.088
24. Taira, S., Nakashima, K., Mori, K., 1993. Kinetic Behavior of Dissolution of Sintered Alumina Into CaO-SiO_2&Al_2O_3 Slags. ISIJ Int. 33, 116–123. https://doi.org/10.2355/isijinternational.33.116
25. Choi, J.-Y., Lee, H.-G., Kim, J.-S., 2002. Dissolution rate of Al_2O_3 into molten CaO-SiO_2-Al_2O_3 slags. ISIJ Int. 42, 852–860. https://doi.org/10.2355/isijinternational.42.852
26. SAMADDAR, B.N., KINGERY, W.D., COOPER, A.R., 1964. Dissolution in Ceramic Systems: 11, Dissolution of Aluminu, Mullite, Anorthite, and Silica in a Calcium-Aluminum-Silicate Slag. J. Am. Ceram. Soc. 47, 249–254. https://doi.org/10.1111/j.1151-2916.1964.tb14405.x
27. OISHI, Y., COOPER, A.R., KINGERY, W.D., 1965. Dissolution in Ceramic Systems: III, Boundary Layer Concentration Gradients. J. Am. Ceram. Soc. 48, 88–95. https://doi.org/10.1111/j.1151-2916.1965.tb11805.x

28. Bui, A.-H., Ha, H.-M., Kang, Y.-B., Chung, I.-S., Lee, H.-G., 2005. Dissolution behavior of alumina in mold fluxes for steel continuous casting. Met. Mater. Int. 11, 183–190. https://doi.org/10.1007/BF03027440
29. Cho, W.D., Fan, P., 2004. Diffusional Dissolution of Alumina in Various Steelmaking Slags. ISIJ Int. 44, 229–234. https://doi.org/10.2355/isijinternational.44.229
30. R. H. Petrucci., W. S. Harwood., 1993. General Chemistry, 6th ed., Macmillan, New York, 535.
31. Liu, Y.Q., Wang, L.J., Chou, K.C., 2014. Dissolution behavior of Al2O3 in refining slags containing Ce2O3. ISIJ Int. 54, 728–733. https://doi.org/10.2355/isijinternational.54.728